Astro2020 Science White Paper

High Angular Resolution Astrophysics in the Era of Time Domain Surveys

Thematic Areas: ☐ Planetary Systems ☐ Star and Planet Formation
☐ Formation and Evolution of Compact Objects ☐ Cosmology and Fundamental Physics
☒ Stars and Stellar Evolution ☐ Resolved Stellar Populations and their Environments
☐ Galaxy Evolution ☐ Multi-Messenger Astronomy and Astrophysics

Principal Author:
Name: Gail H. Schaefer
Institution: The CHARA Array of Georgia State University, Mount Wilson, CA 91023, USA
Email: schaefer@chara-array.org
Phone: 1-626-500-0012

Co-authors:
Arnaud Cassan (Institut d'Astrophysique de Paris, Sorbonne Université)
Robert Klement (The CHARA Array of Georgia State University)
Stephen Ridgway (NOAO)
Theo ten Brummelaar (The CHARA Array of Georgia State University)

Abstract:

Over the next decade, all-sky photometric surveys will dramatically increase the number of transient events, variable stars, and exoplanets discovered. Long-baseline optical interferometry has the power to resolve the spatial structure of bright time variable sources. These direct observations can be compared with the physical properties and models inferred from the photometric light-curves and spectroscopic variations. Transient observations that are particularly well-suited for interferometric follow-up include measuring the angular expansion and spatial structure during the early stages of novae outbursts, mass ejections in Be stars, and gravitational microlensing events. For short-lived transient events, it is critical for interferometric arrays to have the flexibility to respond rapidly to targets of opportunity and optimize the selection of baselines and beam combiners to provide the necessary resolution and sensitivity to resolve the source as its brightness and size change over time.

Introduction

Time domain surveys play an increasingly important role in astronomy, leading to numerous discoveries of transiting exoplanets, variable stars, and transient events. Long-baseline optical interferometry provides an opportunity to spatially resolve transient events to investigate how their structure changes over time. This paper focuses on the advantage of following up bright transient events such as novae, outbursting Be stars, and gravitational microlensing events at high angular resolution.

Angular Expansion and Asymmetries in Novae Explosions

A classical nova occurs when material accreting onto the surface of a white dwarf in a close binary system ignites in a thermonuclear runaway (Bode & Evans, 2008). Studying the structure of novae during the earliest phases requires spatial resolutions on the order of milli-arcseconds. Long baseline interferometry can measure the size and expansion of novae as early as days to weeks after the explosion. This has been accomplished for seven bright novae using interferometers in operation over the past couple of decades (see review by Chesneau & Banerjee, 2012). About three classical novae are detected per year in the galaxy (Warner, 2008), and only about one per year is brighter than $V = 6-8$ mag at the peak brightness, in the sensitivity range of current interferometers. Upcoming all sky surveys could increase the number of Galactic novae detected per year. Similarly, improvements in the sensitivity and resolution of existing and future interferometers will increase the number of novae that can be observed interferometrically.

The angular expansion curve and reconstructed images of Nova Del 2013 are shown in Figure 1 (Schaefer et al., 2014). Changes in the apparent expansion rate can be explained by a model consisting of an optically thick core surrounded by a diffuse envelope. The optical depth changes as the ejected material expands and cools. Studying the structure of novae at the earliest stages provides a way to test theoretical models of novae eruptions. Interferometric observations indicate that elliptical asymmetries can develop as early as a few days after the outburst, suggesting that the explosions might be inherently bipolar (Orio & Shaviv, 1993; Porter et al., 1998; Scott, 2000) or that the elliptical shape develops early during the common envelope phase (Livio et al., 1990; Lloyd et al., 1997). Additionally, the angular expansion rate can be combined with radial velocity

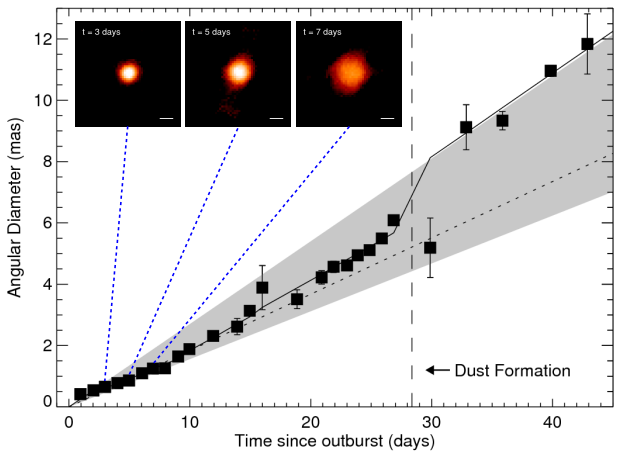

Figure 1: Angular expansion of Nova Del 2013 from Schaefer et al. (2014). The measured angular diameters in milli-arcseconds are plotted against the day of observation following the detonation. Changes in the expansion rate reveal how the structure of the ejected material evolves as the gas expands and cools. The three inserted panels the fireball as imaged with the CHARA Array on days 3, 5, and 7 after the explosion. The horizontal bar at the bottom right of each image corresponds to an angular size of 0.5 milliarcseconds ($\sim$ 2.3 AU).

measurements to derive a geometric distance to the nova. Multi-wavelength interferometric observations can reveal wavelength dependent changes in the optical depth of the expanding material; whereas imaging in the mid-infrared can shed light on where dust formation occurs.

Be Star Outbursts

Classical Be stars are rapidly rotating **B**-type stars showing characteristic line **e**mission, which originates from gaseous circumstellar decretion disks (cf. accretion disks) rotating close to Keplerian way (Rivinius et al., 2013). The disk is formed by mass being ejected from the central star, and with a sufficient mass ejection rate, the disk ends up growing outwards due to anomalous viscosity of the same type that operates in the more famous accretion disks. Under the condition of a steady mass ejection for a sufficiently long time, the disk eventually settles into a steady state, while transporting mass and angular momentum into the interstellar medium. However, rather than being stable over long periods of time, most Be stars show variability in most observables on various timescales.

While the physical properties of many Be disks are quite well understood in the context of viscous decretion, the nature of the mass ejection mechanism itself is poorly understood. Rotation rates are generally thought to be close to but below the critical limit, in which thermal motions on top of rotation would be sufficient to eject material into orbit. On the contrary, an additional mechanism on top of rotation seems to be needed, and the currently most accepted mechanisms are non-radial pulsations, small scale magnetic fields, or a combination of the two. The observational signatures of ejection of mass from the central star differ widely from star to star. There are examples of the mass ejection being seemingly perfectly steady (e.g., β CMi; Klement et al., 2015), while others show episodic behavior of mass ejection, i.e., outbursts (Labadie-Bartz et al., 2018, and references therein). These outbursts occur periodically or quasi-periodically in some stars, while in many others the outburst occurrence is irregular. Resolving the geometry and temporal evolution of these outbursts is crucial for advancing our understanding of the nature of mass ejection in Be stars.

Be star outbursts are well observable by spectroscopy as a sudden increase in line emission and onset of line asymmetry (e.g., Rivinius et al., 1998), in photometry as a sudden change in observed magnitude (e.g., Ghoreyshi et al., 2018), and in linear polarimetry as a sudden change in polarization percentage and/or position angle (Carciofi et al., 2007). Figure 2 shows an example of an outbursting Be star. These all suggest the outbursts are likely localized events, after which a period of time is needed for the material to settle into circular orbit. Interferometric observations of Be stars are the origin of significant milestones achieved in our understanding of these objects, such as the first direct confirmation of disk-like geometry of the circumstellar matter (Quirrenbach et al., 1994), Keplerian rotation of the disk (Meilland et al., 2007), and even the presence of one-armed density waves propagating through the disk (Carciofi et al., 2009). Being able to image (or at least angularly resolve) the geometry of a Be star outburst from its initial phases to the settling of the material into orbit is very likely to bring another such milestone by constraining the crucial properties of the mass ejection mechanism acting on top of rapid rotation.

Currently, the optical interferometric facility with highest achievable angular resolution - the CHARA Array - is at the limit of being able to image strong outbursts for Be stars showing outburst behavior. The most promising candidates, such as o And or θ CrB, are just below the resolution limit of the main CHARA imaging instrument MIRC-X (angular resolution in H-band continuum

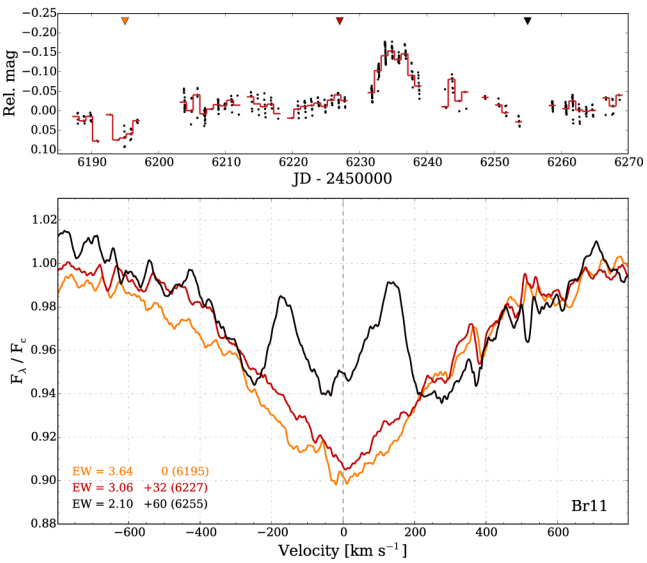

Figure 2: Outburst of the B5V star ABE-098 (HD 219523) from Labadie-Bartz et al. (2018). *Top:* KELT light curve showing the outburst. *Bottom:* APOGEE spectra showing the Br11 line. The color-coding of each spectrum corresponds to the times marked by the orange, red, and black triangles in the upper panels before and after the outburst.

of $\sim$ 0.5 mas), so that only an outburst of huge magnitude would be possibly resolved. Other promising targets are just below the current sensitivity limit. Clearly, an improvement in angular resolution (longer baselines) and/or sensitivity is needed for actual imaging of the outburst of a Be star. Nevertheless, there are ongoing spectroscopic and photometric monitoring campaigns focusing on outbursting Be stars, some of them in collaboration with the CHARA Array itself in order to trigger possible follow-up interferometric observations even with the current capabilities.

Microlensing Events

Gravitational microlensing occurs when light rays from a background (bulge) star bend as they pass close to the line-of-sight of a foreground (lens) star (e.g., Paczynski, 1996). The time variable magnification of the distant star can be measured photometrically. Gravitational microlensing offers a unique opportunity to detect exoplanet and brown dwarf companions around the lens star, free-floating exoplanets, and compact objects such as Galactic stellar mass black holes (Paczynski, 1986; Mao & Paczynski, 1991; Sumi et al., 2011; Cassan et al., 2012; Gaudi, 2012; Ranc et al., 2015).

During a microlensing event, the source splits into several images of different sizes and whose angular separations are typically on the order of a milli-arcsecond. While the photometric light curve of a microlensing event provides important constraints on the lens physical parameters, in many cases the lens mass and distance from Earth remain degenerate. Long-baseline interferometric observations of microlensing events combined with the modeling of the light curve can break this degeneracy, and also provide the motion of the lens relative to the source. This can be done in two ways. First, interferometry can be used to resolve the individual images of the source star (Delplancke et al., 2001; Rattenbury & Mao, 2006). Alternatively, if the images are not resolved, narrow-angle astrometry could be used to measure the astrometric displacement of the image photocenter; the wobble signature would be on the order of a few hundred micro-arcseconds (e.g., Han, 2002; Dalal & Lane, 2003).

Figure 3 illustrates simulations of measuring the two-dimensional separation between two images of a microlensing event created by a typical single lens (Cassan & Ranc, 2016). The separation

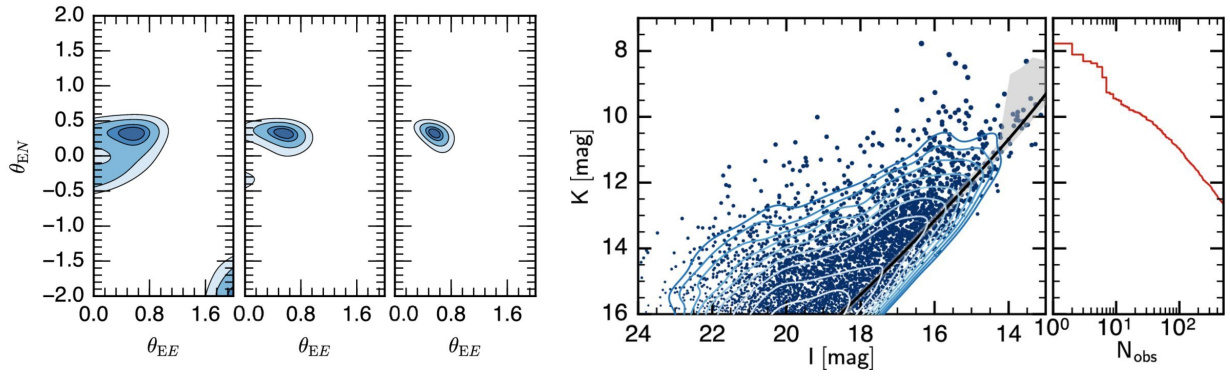

Figure 3: *Left:* Simulated interferometric measurements showing the confidence contours ($1-4\,\sigma$) for the Einstein radius $\theta_{\rm E}$ in the North and East directions ($\theta_{\rm E,N}$ =0.325 mas, $\theta_{\rm E,E}$ = 0.563 mas). The three panels from left to right show the improvement in the source characterization for one, two, and three interferometric observations using squared visibilities on six baselines (Cassan & Ranc, 2016). *Right:* Predicted K magnitude at peak for microlensing events alerted by OGLE in 2011−2014 (blue dots) as a function of the baseline I magnitude, taking into account magnification, reddening, and lens-source de-blending. The right-most panel shows a cumulative histogram of the number of events that have a peak K magnitude lower than threshold K (Cassan & Ranc, 2016).

between the lensed images is characterized by the Einstein radius $\theta_{\rm E}$. The simulations were based on the VLTI PIONIER instrument which combines the light from the four Auxiliary Telescopes, leading to six simultaneous baselines. The results show that good constraints can be obtained with two measurements, however, a third observation improves the results, especially when the brightness of the source is close to the sensitivity limit of the instrument. Moreover, observations at three epochs could reveal the displacement of the multiple images over time.

Microlensing events suitable for interferometric observations can be triggered based on real-time analysis of the photometric light curves monitored by networks of telescopes. Real-time modeling shows that a reasonable prediction of the date and brightness of the peak magnification can be obtained two or three days in advance of the peak, providing 48 h to issue a Target of Opportunity alert (Cassan & Ranc, 2016). New generations of alert telescopes in operation since 2011 have increased the rate of microlensing event detections from a few hundreds to more than 2000 per year. Figure 3 shows the predicted peak K-band magnitudes of OGLE microlensing events detected in 2011−2014 computed by Cassan & Ranc (2016). The first potential target appears at $K \sim 7.8$, while 26 events have $K \leq 10$ (hence, a mean of 6−7 per year). These magnitudes are within reach of VLTI using either the Unit Telescopes (UT, 8 m) or the Auxiliary Telescopes (AT, 1.8 m). An increase by only one magnitude in sensitivity would provide an order of magnitude more microlensing targets for the next generation of instruments.

The two images from a microlensing event have been resolved successfully for the first time using the VLTI GRAVITY beam combiner (Dong et al., 2019). The current number of microlensing alerts (about 2000 per year delivered by OGLE IV) and the capabilities of the new generation of robotic telescopes working in network (like the RoboNet collaboration) have greatly improved the ability to detect and follow-up suitable targets for interferometric observations. Recent im-

provements in the sensitivity of long baseline interferometers have opened up new possibilities to observe microlensing events. Several microlensing events per year are already within reach. Interferometric microlensing observations carry great promise to characterize completely many more microlensing systems in the near future. Improved sensitivity of U.S. based interferometers like the CHARA Array, the Navy Precision Optical Intereferometer, and the upcoming Magdalena Ridge Observatory Interferometer, would increase the number of microlensing events that could be monitored in the coming years.

Recommendations for the Astro2020 Decadal Survey

Bright transient events discovered by sky surveys (e.g., RoboNet collaboration, OGLE, Zwicky Transient Facility) can be followed up interferometrically to measure the spatial extent of the source. Rapidly responding to transient events requires interferometric facilities to build a mechanism for handling target of opportunity requests. In addition to scheduling the observations, this requires the flexibility to optimize the selection of baselines and beam combiners to match both the resolution and sensitivity needed to resolve the source as its size and brightness change over time. Improvements in the sensitivity of interferometers down to $K \sim 10$ mag and/or improvements in spatial resolution by building longer baselines would increase the number of transient events that could be resolved spatially.

References

Bode, M. F., & Evans, A. 2008, Classical Novae (Cambridge: Cambridge University Press)

Carciofi, A. C., Magalhães, A. M., Leister, N. V., Bjorkman, J. E., & Levenhagen, R. S. 2007, ApJL, 671, L49

Carciofi, A. C., Okazaki, A. T., Le Bouquin, J.-B., et al. 2009, A&A, 504, 915

Cassan, A., & Ranc, C. 2016, MNRAS, 458, 2074

Cassan, A., Kubas, D., Beaulieu, J.-P., et al. 2012, Nature, 481, 167

Chesneau, O., & Banerjee, D. P. K. 2012, Bulletin of the Astronomical Society of India, 40, 267

Dalal, N., & Lane, B. F. 2003, ApJ, 589, 199

Delplancke, F., Górski, K. M., & Richichi, A. 2001, A&A, 375, 701

Dong, S., Mérand, A., Delplancke-Ströbele, F., et al. 2019, ApJ, 871, 70

Gaudi, B. S. 2012, ARA&A, 50, 411

Ghoreyshi, M. R., Carciofi, A. C., Rímulo, L. R., et al. 2018, MNRAS, 479, 2214

Han, C. 2002, ApJ, 564, 1015

Klement, R., Carciofi, A. C., Rivinius, T., et al. 2015, A&A, 584, A85

Labadie-Bartz, J., Chojnowski, S. D., Whelan, D. G., et al. 2018, AJ, 155, 53

Livio, M., Shankar, A., Burkert, A., & Truran, J. W. 1990, ApJ, 356, 250

Lloyd, H. M., O'Brien, T. J., & Bode, M. F. 1997, MNRAS, 284, 137

Mao, S., & Paczynski, B. 1991, ApJL, 374, L37

Meilland, A., Stee, P., Vannier, M., et al. 2007, A&A, 464, 59

Orio, M., & Shaviv, G. 1993, Ap&SS, 202, 273

Paczynski, B. 1986, ApJ, 304, 1

Paczynski, B. 1996, ARA&A, 34, 419

Porter, J. M., O'Brien, T. J., & Bode, M. F. 1998, MNRAS, 296, 943

Quirrenbach, A., Buscher, D. F., Mozurkewich, D., Hummel, C. A., & Armstrong, J. T. 1994, A&A, 283, L13

Ranc, C., Cassan, A., Albrow, M. D., et al. 2015, A&A, 580, A125

Rattenbury, N. J., & Mao, S. 2006, MNRAS, 365, 792

Rivinius, T., Baade, D., Stefl, S., et al. 1998, A&A, 333, 125

Rivinius, T., Carciofi, A. C., & Martayan, C. 2013, A&A Rv, 21, 69

Schaefer, G. H., ten Brummelaar, T., Gies, D. R., et al. 2014, Nature, 515, 234

Scott, A. D. 2000, MNRAS, 313, 775

Sumi, T., Kamiya, K., Bennett, D. P., et al. 2011, Nature, 473, 349

Warner, B. 2008, in Classical Novae, ed. M. F. Bode & A. Evans, Classical Novae (Cambridge: Cambridge University Press), 16–33